Original article

Stability determinants of bone-borne force-transmitting components in three RME hybrid expanders—an *in vitro* study

Andre Walter[1], Brigitte Wendl[2], Oliver Ploder[3], Sergi Mojal[4] and Andreu Puigdollers[1]

[1]Department of Orthodontics and Dentofacial Orthopaedics, School of Dentistry, Universitat Internacional de Catalunya, Barcelona, Spain, [2]Department of Clinical Orthodontics, Medical University Clinic, Graz, Austria, [3]Department of Oral and Maxillofacial Surgery, Academic Teaching Hospital, Feldkirch, Austria and [4]Statistical analysis and research, Instituto municipal de Investigaciones Médicas (IMIM), Hospital del Mar d´Investigaciones Mèdiques, Barcelona, Spain

Correspondence to: Andreu Puigdollers, Universitat Internacional de Catalunya, Campus Sant Cugat, Josep Trueta s/n, 08195 Sant Cugat del Vallès, Barcelona, Spain. E-mail: apuigdollersp@gmail.com

Summary

Background: The aim was to test which component [wire arm, connecting abutment attachment, and orthodontic mini-implant (OMI)] of the force-transmitting system (FTS) in the anterior palate of three commonly used hybrid expanders (HEs; WILMES-HE, LUDWIG-HE, and WINSAUER-HE) deforms under increasing load.
Materials and methods: Crude single and double wire arms were tested individually. Non-opening of the maxillae halves was simulated in artificial bone blocks with single wire and double wire FTS specimens. OMIs were inserted 8 mm and underwent 6 mm of continuous static lateral loading. Deformation angles were measured (X-ray, $n = 6$) at 0, 3 and 6 mm feed. OMIs and abutments were scan electron microscope (SEM) evaluated.
Results: After 1.0 mm of loading, the single wire arm of all FTS deformed between 63.4 (16.5) N and 76.2 (18.4) N, and the double wire arm of reinforced FTS (wires positioned 'side by side') deformed after 1.0 mm between 110.0 (18.4) N and 134.8 (22.3) N. The crude single wire resisted 89 (5.1) N until plastic deformation, whereas the crude double wire positioned 'on top of each other' resisted 438 (21.3) N. At 6 mm loading, the reinforced WINSAUER-HE FTS withstood a maximum load of 320.9 (31.1) N and the reinforced LUDWIG-HE FTS 19% less, both under great deformation of double wires and OMIs. The screw-fixated WILMES-HE FTS abutment attachment (overlapping OMI head 34%) detached around 250 N. The bonded WINSAUER-HE and LUDWIG-HE abutment attachments did not detach. Nor did the modified bonded plus the modified screw-fixated WILMES-HE abutment attachment when overlapping 100%.
Conclusion: Early OMI and single wire arm deformation in HEs are crucial for unsuccessful RME in more mature maxillae. Double wire arms should be obligatory. OMIs with inner diameter greater 1.36 mm are recommended. One hundred per cent overlapping abutment attachments do not detach.

Introduction

More than 150 years ago, Angell split the maxilla (non-surgically) in sagittal direction along the median suture and expanded it bilaterally in a case exhibiting a transverse deficiency (1). This technique of rapid maxillary expansion (RME) was popularized by Haas (2) in the 1960s. Since then maxillary expansion has been carried out with

tooth-borne appliances using various expansion protocols. The outcome is a significant widening of the palatal dome (3). Wehrbein *et al.* (4) pioneered the use of palatal implants for orthodontic procedures. These implants were short and thick ('Orthosystem', Institut Straumann, Waldenburg, Switzerland, diameter 3.3 mm, length 4 or 6 mm) and required surgical implantation and explanation making it unfeasible for routine anchorage of maxillary expanders.

Today the so-called hybrid expanders (HEs anchored on two orthodontic mini-implants (OMIs) in the anterior palate and on the first upper molars are increasingly used for rapid maxillary expansion in children and preadolescents (5) (Figure 1a–c). This anchorage also prevents first molar mesial movement until the other permanent buccal teeth have erupted. Three types of HEs with bone-borne anchorage in the anterior palate with different abutment attachments and different OMIs were described by WILMES (6, 7), LUDWIG (5) and WINSAUER (8). Another form of a HE is the maxillary skeletal expander (M.S.E., Biomaterials Korea). It is anchored on 4 OMIs in the posterior palate and dentally on the first two molars (9). Lagravère *et al.* (10) published a bone-borne expander on two implants and OMIs (diameter 1.5 mm) placed in the posterior palate.

The force-producing system (FPS; expansion screw) transmits its force via the force-transmitting system (FTS) into the maxilla halves (Figure 2a and 2b). The anterior arms deliver the force to the OMIs in the anterior palate, while the posterior arms transmit the force to the molars in the posterior section of the palate. The posterior single fastening wires are laser welded to molar bands as additional tooth-borne anchorage. The three anterior components (anterior wire arms, abutment attachments and OMIs) are bone-borne and transmit the expanding force as a cantilever arm directly into the maxillary bone (Figure 2a). The force of these components and their generated moments against the withstanding force of the maxilla especially when used in more adult patients has yet not been investigated.

The aim of this *in vitro* study was to evaluate which components of the anterior FTS in the anterior palate of three different types of HEs deform most under maximum stress.

Materials and methods

This *in vitro* study investigates the loading behaviour and the morphology of the anterior FTSs of expanders with their bony anchorage placed in the anterior palate where bone heights are between 8 and 5 mm (11–14). Three hybrid-type expanders met the inclusion criteria of anterior palate bone-borne anchorage with OMIs: the WILMES-HE, the LUDWIG-HE and the WINSAUER-HE. Other maxillary expanders were excluded (M.S.E. and the Lagravère expander) (9, 10), as their bony anchorage is located in the (i) posterior palate and (ii) comprising bone heights less than 5–8 mm (15).

The WILMES group (6) connects the anterior single wire arms of the HE with two paramedian OMIs [diameter 2.0 mm, total screw length 14.0 mm, threaded from tip to neck; (Benefit Orthodontic screw, PSM-company, Tuttlingen, Germany)] in the anterior palate with pre-drilling prior to insertion. Abutment attachments are laser welded laterally to the anterior wire arms of the HE and connected to the OMIs by means of an internal fixation screw with a proprietary short manual screwdriver. After loosening the molar bands and opening the internal fixation screws, the HE can easily be removed, thus offering the option to use the OMIs for other procedures [e.g. extrusion of impacted teeth, intrusion, distalization and mesialization of molars or even the use of a greater dimensioned HE, if necessary (16)].

The LUDWIG group has modified this method by using self-drilling OMIs (Orthoeasy®, Forestadent, Pforzheim, Germany, diameter

1.8 mm, total screw length 14.0 mm, threaded from tip to neck) and self-curing composite for the bonded fixation (Phase II, Reliance® orthodontic products, Itasca, Illinois, USA) of the abutment caps (Figure 1b). The anterior single wire arms are welded on top of the abutment caps (5). However, the irreversibility of the abutment–OMI fixation could be of disadvantage, since for the removal of the HE the anterior expander arms have to be cut, leaving the bonded abutment attachments on the head of the OMIs. For removal of the
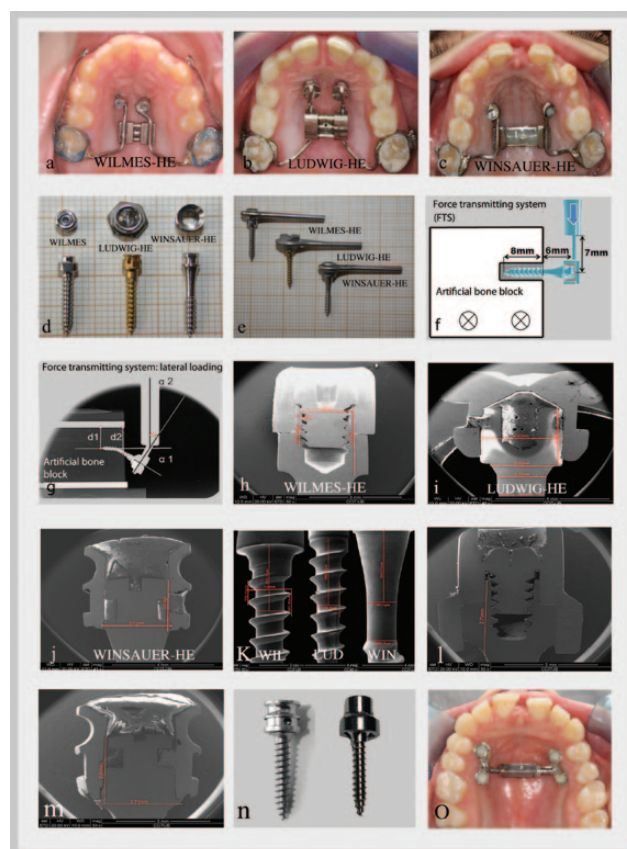
Figure 1. Three different types of hybrid expanders (HEs) with their anterior force transmitting components: single anterior wire arms with abutment attachments and orthodontic mini-implants (OMIs). (a) WILMES design HE with screw-fixated abutment attachments (PSM) and their OMIs (PSM). (b) LUDWIG design HE with OMIs (Forestadent) and bonded abutment caps (Forestadent). (c) WINSAUER design HE with OMIs (Jetscrew, Jeil Medical) and bonded abutment collars (Tiger Dental). (d) OMIs and their abutments attachments prior to fixation. (e) Samples with abutment attachments bonded or screw fixated to OMI heads and with double anterior wire arms. (f) Setting of the 'force-transmitting system' in artificial bone. (g) X-ray imaging in artificial bone block displays deformation of double wire arm and OMI during static loading simulating RME in not separating maxilla halves (maximum stress). (h, i, j) Scan electron microscope (SEM) cross-sectional images and measurements of the OMI head specimens with the abutment attachments fixated on them. (k) SEM image of the OMIs shanks 3 mm below their neck. (l) SEM cross-sectional image of the WILMES-HE OMI head and the modified 100% overlapping screw-fixated WILMES-HE-LSA (lengthened screw-fixated abutment). (m) SEM cross-sectional image of the slightly modified WILMES-HE OMI head and the modified, 100% overlapping, bonded WILMES-HE-LBA (lengthened bonded abutment). (n) Macroscopic view of the 'screw-fixated version' and 'bonded version' abutments attachments with PSM OMIs. (o) Pure bone-borne expander (MICRO-4) placed on 4 OMIs (Jet screw, Jeil Medical) and bonded abutment collars (Tiger Dental) connected to reinforced double wire arms.
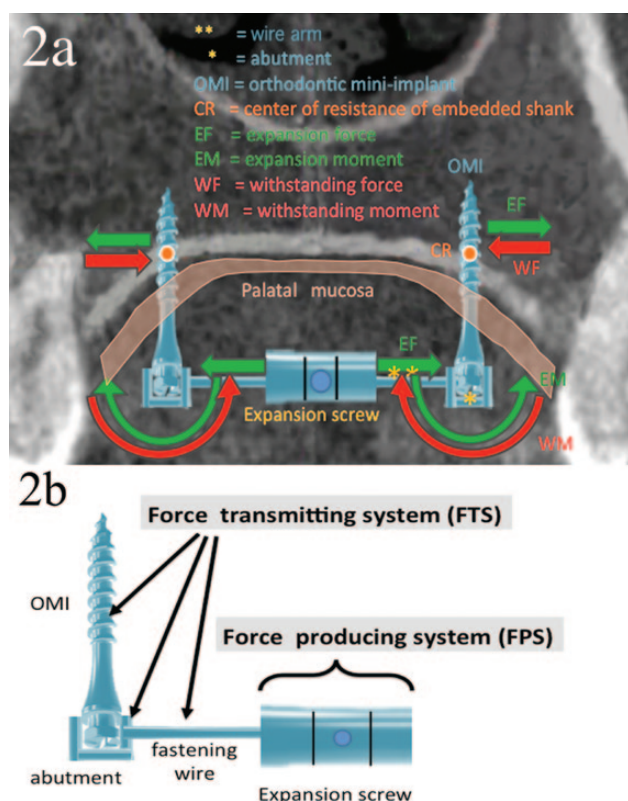
Figure 2. Schematic illustration of moments and forces of the force-transmitting system (FTS) of hybrid expanders (HEs) during maxillary expansion. (a) Generation of moments and forces under maximum stress. (b) Components of the FTS and force-producing system (FPS).

abutment attachments, the OMIs have to be removed as well, leaving no possibility to use them afterwards for other purposes.

The WINSAUER group (8) also uses self-curing composite to cement the collar-type abutment attachments (Tiger Dental, Bregenz, Austria) onto self-drilling OMIs placed bilaterally in the anterior palate (Dual Top, Jet screw, Jeil Medical, Seoul, Korea, diameter 2.0, total screw length 14.5 mm; Figure 1c). For luting, a bonding composite (Phase II, Reliance® orthodontic products, Itasca, Illinois, USA) is injected with a syringe between the collar and the head of the OMI. Air bubbles and surplus composite are released via a drain hole in the collar, which practically guarantees a complete 'fill' of the connection. The Jet screw was specially designed for placement in the anterior palate. Its shank differs from that of other OMIs by having three sections (Figure 1d): a 7.0 mm lower threaded section followed by a 2.0 mm middle thread-free cylindrical section and an upper thread-free conical section. The lower threaded section and the middle thread-free section have the same shank diameter. This allows the middle thread-free section of the shank to be screwed into the bone without resistance, whereas the upper section compresses the surrounding gingiva as the diameter there increases. The collar-type abutment attachment can easily be removed by means of a proprietary collar extractor (8), allowing the OMIs to stay in place fully intact and to be used for further procedures like anchoring a distalizer or a bonded transpalatal arch as a long-time retention.

All the OMIs were manufactured from titanium alloy (Ti 6Al-4V ELI). The OMIs and the abutment attachments (cap, collar) are shown in Figure 1d before and in Figure 1e after fixation.

Crude wire pretest

In conventional use, the connection between the HE expansion screw and the OMI's abutment attachment are single stainless steel wire arms. The anterior and posterior wire arms of common expansion screws used in these HEs have a diameter between 1.48 and 1.49 mm (17). For variable control, all wires used in this study were 1.49 mm diameter stainless steel wires (Remanium®, round, hard, 513-150-00, Dentaurum, Ispringen, Germany).

When testing FTSs, each of the three components (wire arms, abutment attachment and OMI) represents a variable. For variable control, the wires were therefore pretested separately for more information. Due to early plastic deformation of the crude single wire, a second crude wire was added to the single wire in order to obtain higher loading results. The bending behaviour of crude single and double wires was pre-evaluated ($n = 3$) in two ways with three-point flexural tests (Table 1a). First, a three-point flexural pretest with mandrel was carried out, where the deformation characteristics of crude specimen single wire and double wires (positioned 'side by side'; Figure 3a and 3b) were investigated according to ISO Norm 15841:2006 (distance between supports 15.0 mm, radius of bending mandrel 1.5 mm). The crude single wires started to deform after 1.0 mm at a force of 81 (4.2) N, the crude double wire 'side by side' after 1.1 mm at a force of 159 (7.3) N, respectively (Figure 3c).

Thereafter, a three-point flexural pretest with a hyrax screw (distance between supports 15.0 mm) was performed to be able to also test laser fixated double wires positioned 'on top of each other' in an expansion screw (Superscrew™, SUPERscrewSUPERspring Co, Highwood, Illinois, USA). These wires were laser welded to each other lengthwise for maximum stability. In the regular three-point flexural pretest with mandrel, these double wires positioned on top of each other could not be tested due to position changes. For comparison, a single wire was also tested this way (Figure 4a–c). The single wire in the hyrax screw testing assembly started to deform after 1.2 mm at a force of 89 N (5.1), the double wires ('on top of each other') after 1.4 mm at a force of 438 N (21.3), respectively. With plastic deformation after 3 mm of central bending, a force of 561 N (27.2) was measured.

The early wire deformation in the crude single wire pretests led to the author's decision that besides single wire FTSs (standard) also double wire FTSs (reinforced) should be tested. For these reinforced FTSs, we decided to use double wires 'side by side', because this wire arm design can easily be applied to HEs in clinical use. This extended study design eliminated a weak spot by creating greater stability to the FTS and hence straining the other components (abutment attachment and OMI) more evenly. The stability of FTS with wire arms positioned 'on top of each' other should be evaluated in a further study.

General setting for FTS tests

In order to simulate a 'non-opening suture', the artificial bone blocks were kept stable, while a continuous static unilateral load was applied to each of the three FTS types. Of the three different FTS types, one set with standard single wire arms ($n = 6$) as used in standard expansion screws and another set with reinforced double wire arms ($n = 10$) were investigated (Figure 3d–f). Wire arms were made of a single 27 mm long, 1.5 mm diameter stainless steel wire (Dentaurum, Ispringen, Germany), respectively, double wires positioned 'side by side'. They were laser welded bilaterally to the abutment attachments (Figure 1e). Force values were measured at 1, 3 and 6 mm and evaluated statistically. Thereof, the resulting moments were calculated. In the mouth, this would correspond to a bilateral

Table 1. Pretest on crude wire plastic deformation (three-point flexural test) and FTS load-bearing capacity (6 mm lateral loading test) of the three HE systems. N = Newton; HE = hybrid expander; FTS = force-transmitting system; OMI = Orthodontic mini-implant; d1 = distance from reference line to OMI tip; d2 = distance from reference line to OMI shaft center on the surface block.

	n	Mean N (SD)	Mean N (SD)	Mean N (SD)	*P*-values*		
a) Three-point flexural pretest with mandrel (above) and three-point flexural pretest with hyrax expansion screw (below): before plastic deformation							
crude single wire	3	81 (4.2) N at 1.0 mm	mean (SD)		—	—	—
crude double wires (side by side)	3	159 (7.3) N at 1.1 mm	mean (SD)		—	—	—
Hyrax screw single wire	3	89 (5.1) N at 1.2 mm	mean (SD)		—	—	—
Hyrax screw double wires (on top of each other)	3	438 (21.3) N at 1.4 mm	mean (SD)		—	—	—

		WILMES-HE	LUDWIG-HE	WINSAUER-HE	WINSAUER-HE versus LUDWIG-HE	WILMES-HE versus WINSAUER-HE	LUDWIG-HE versus WILMES-HE
b) FTS static loading test (standard single wire arm)							
at 1 mm	6	73.4 (18.3)	63.4 (16.5)	76.2 (18.4)	0.481	0.845	0.269
at 3 mm	6	115 (15.1)	87.3 (10.4)	114.3 (17.4)	0.008	0.815	0.016
at 6 mm (maximum)	6	**158.8 (11.3)**	**112.0 (8.9)**	**158.3 (12.4)**	**<0.001**	**0.997**	**<0.001**
c) FTS static lateral loading test (reinforced, double wire arm, side by side)							
at 1 mm	10	130.6 (19.7)	110.0 (18.4)	134.8 (22.3)	0.028	0.810	<0.001
at 3 mm	10	254.2 (25.8)	209.2 (31.5)	271.3 (31.8)	<0.001	0.417	0.006
at 6 mm (maximum)	10	—	**260.9 (44.0)**	**320.9 (31.1)**	**0.002**	—	—
d) OMI displacement (d1 tip, d2 shank, reinforced, double wire arm, side by side)		mm	mm	mm			
X-rayd1 at 3 mm	6	–0.28 (0.23)	–0.02 (0.04)	–0.57 (0.14)	<0.001	0.018	0.026
X-rayd1 at 6 mm	6	—	–0.08 (0.24)	–1.07 (0.15)	<0.001	—	—
X-rayd2 at 3 mm	6	1.43 (0.37)	1.47 (0.41)	1.30 (0.23)	0.684	0.782	0.985
X-rayd2 at 6 mm	6	—	3.20 (0.47)	3.05 (0.37)	0.553	—	—
e) OMI shank deformation (α1) and reinforced double wire (side by side) deformation (α2)		Degree	Degree	Degree			
X-rayα1 at 3 mm	6	16.0 (2.28)	19.8 (2.04)	14.0 (1.41)	<0.001	0.210	0.010
X-rayα1 at 6 mm	6	—	37.8 (2.48)	27.0 (2.97)	<0.001	—	—
X-rayα2 at 3 mm	6	9.17 (2.48)	14 (2.1)	12.67 (1.03)	0.487	0.020	0.002
X-rayα2 at 6 mm	6	—	30.0 (2.53)	26.8 (3.19)	0.086	—	—

The 6 mm values were calculated with a Student's *t*-test for independent samples.

*P-values were calculated using a Tukey's multiple comparison correction in ANOVA, except data at 6 mm.
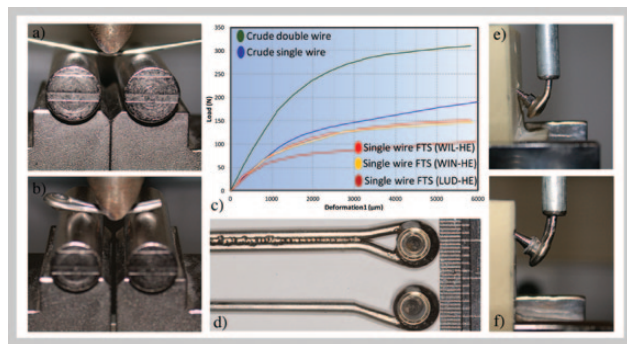
Figure 3. Three-point flexural pretest of crude single and double wire arms and loading test of force-transmitting system (FTS) with mandrel. (a) Pretest of crude standard single wire. (b) Pretest of crude double wire ('side by side'). (c) Median value graphs of three-point flexural pretest with mandrel of crude single and double wire. Mean loading values of all tested single wire FTSs. (d) FTS samples with single and double wire. (e) Single wire FTS sample (WILMES-HE) after 6 mm of loading. (f) Double wire 'side by side' FTS sample (WINSAUER-HE) after 6 mm of loading.

opening of the Jackscrew of 2, 6 and 12 mm without separation of the maxilla halves. This setting closely mimics RME conditions when the expansion screw is opened without concomitant suture opening. Under these conditions, OMIs are displaced or clinically undergo great deformation due to the generated forces and moments (18). In clinical reality after 3 mm of expansion, the suture should open or else the expansion would be stopped or assisted surgically. Otherwise components of the appliance would deform permanently and this situation would represent great danger for the patient. As an *in vitro* study, the limitation of the weakest component could be explored easily without causing harm to patient.

Orthodontic mini-implants

The OMIs were inserted (i) without pre-drilling into artificial bone blocks to a depth of 8 mm. This depth was chosen, as this same bone height is also available in the lateral region of the anterior palate (15). The distance between the surface of the artificial bone block and the plane of lateral loading of the FTS was 6 mm (Figure 1f and 1g). This is a representative of the mean thickness of the palatal gingiva around 4 mm (19) and the screw head with its fixed abutment with further 2 mm. The distance from the end of the custom-made Galdabini power arm to the OMI axis was 7.0 mm, reflecting an average length of 7 mm for a HE anterior wire arm (Figure 1f and 1g). The Galdabini loading arm was moved at a speed of 1 mm per 30 seconds, thus gradually increasing the loading force and the moment on the FTS (Figure 1f). The artificial bone blocks consisted of solid rigid polyurethane, simulating a bone density of 0.48 g/cm³ (mean palatal bone density in

adults: 0.45 g/cm³) (20). The density of the artificial bone block was chosen slightly higher to implement the presence of a thin cortical layer.

Mechanical loading tests were conducted using the Galdabini 1890 servo-hydraulic universal testing machine (Galdabini, Cardano al Campo, Italy).

Radiographs

In 6 of the 10 tests, radiographs (Trophy®, Marne-la-Vallée, France) were taken at the beginning and at 3 and 6 mm of lateral loading (Figure 1g). Radiographs of the wire arms, the abutment attachments and the OMIs were taken strictly perpendicular and at a distance of 70 mm from the film. Deformation angles were measured using Adobe Photoshop CS6® software. As an aid to visualize deformation, two reference posts (fiducials, diameter 2.0 mm) were placed parallel above and below the OMI in each artificial bone block. The bottom of the upper fiducial served as a reference line (RFL) to measure deformation and displacement during loading. The lower fiducial served as additional parallax imaging control. d1 represented the distance between the tip of the inserted OMI and RFL, and d2 the distance between RFL and the centre of the OMI shaft measured at the surface of the artificial bone block. Shank deformation was assessed by measuring angle α1 between the OMI's 'head–neck tip' axis before and after loading. Wire arm deformation (α2) was assessed by measuring the angle between the vertical Galdabini power arm and a line perpendicular to the OMI's 'head–neck' axis at the level of the wire arm (Figure 1g).

Scan electron microscope (SEM) images

SEM images (Quantas 200, Oregon, USA) were taken of the attachment in order to measure the overlapping relation (Figure 1h–j) and of the OMIs alone in order to determine the relation between the inner diameter (ID) of the shank and the outer diameter (OD) of the thread (Figure 1k). The inner and outer diameters of the OMI shanks (21), were measured 6 mm below the head of the OMIs. Other measurements were taken from the cross section of the OMIs heads with their abutment attachments bonded or screw fixated to them (cross sections, Figure 1h–j). The OMIs head lengths and the abutment attachments overlapping lengths (AOLs) were measured (accuracy at ×50 and ×100 magnification) and the abutment overlapping portions of the OMI heads (AOP) were then calculated (Table 2). Due to the fact that the LUDWIG-HE and the WINSAUER-HE abutments were bonded and overlapping completely, the original WILMES-HE abutment represented a variable, as it was (i) fixated by an inner screw and (ii) overlapping only partially (Figure 1h).

Variable control

In order to eliminate this variable, the original WILMES-HE abutment was modified (lengthened) by adding (laser welding) the lower part of an original PSM screwdriver, thus achieving complete overlapping. This modified abutment was again screw fixated ('screwed on version') onto the PSM OMI's head, re-evaluated with SEM and tested under static lateral loading (*WILMES-HE-LSA* = WILMES-HE lengthened and screwed on abutment; Figure 1l and 1n). A second version of this complete overlapping abutment, attachment was adapted to be bonded on to the WILMES-HE OMIs head ('bonded version'). To be able to bond this setting, a WINSAUER-HE abutment could be placed onto the WILMES-HE screw head after minimal adaptations of the head diameter (*WILMES-HE-LBA* = WILMES-HE lengthened bonded abutment; Figure 1m and 1n). These two modified abutment attachments then were compared with the original WILMES-HE abutment.

All measurements were carried out by the author Walter Andre. Descriptive statistics with mean and standard deviations (SDs) were calculated for distances, angles and loading forces. Since the Kolmogorov–Smirnov test, Shapiro–Wilk test and Q–Q plots did not indicate lack of normal distribution, analysis of variance with
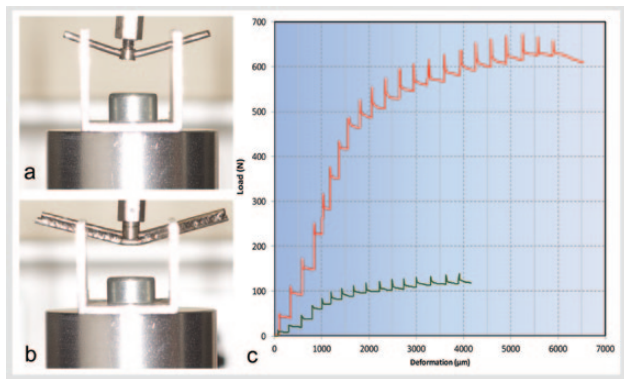
Figure 4. Three-point flexural pretest with expansion screw, single and double wire ('on top of each other'). (a) Hyrax pretest with crude single wire. (b) Hyrax pretest with crude double wire, on top of each other. (c) Results of bending pretest. Green: single wire, red: double wire, on top of each other.

Table 2. SEM data and characteristics of the three different analysed OMIs with their abutment. AOL = abutment overlapped length of the head; AOP = abutment overlapped portion of the head; HE = hybrid expander; OMI = Orthodontic mini-implant; ID = inner OMI diameter (shaft); OD= outer diameter (total); LBA= lengthened bonded abutment; LSA= lengthened inner screw-fixated abutment; SEM = Scan electron microscope.

	Outer diameter (OD; mm)	Inner diameter 6 mm below OMI head (ID; mm)	OMI length (mm)	Thread depth (mm)	*Thread depth/OD ratio	Head length (mm)	AOL (mm)	AOP (%)
WILMES-HE OMI	1.99	1.30	13.70	0.35	35%	2.61	0.89	34%
LUDWIG-HE OMI	1.8	1.05	13.78	0.37	42%	2.62	2.32	89%
WINSAUER-HE OMI	1.99	1.36	14.21	0.31	32%	2.41	2.41	100%
Abutment variables control								
modified WILMES-HE-LSA: screw on version	1.99	1.30	13.70	0.35	35%	2.61	2.61	100%
modified WILMES-HE-LBA: bond-fixated version	1.99	1.30	13.70	0.35	35%	2.81	2.81	100%

*Thread depth/OD ratio (%) = (1–ID/OD) × 100 (i.e. the percentage of the thread depth compared to the outer diameter).

a Tukey's multiple comparison correction was performed to assess differences between the three systems. Data at 6 mm were calculated with the Student's *t*-test for independent variables. *P*-values <0.05 were considered as statistically significant. Statistical analysis was performed with SPSS 18.0 (IBM Corp, New York, USA).

Results

Up to 1.0 mm of static lateral loading, the wire arms of all standard single wire FTSs could be loaded between 63.4 (16.5) N and 76.2 (18.4) N showing only elastic deformation. After 5 more millimetres, the load for the single wire FTSs only increased 77–116 % but at the same time showing major deformations of wires and OMIs (Table 1b; Figure 3c–e). Mechanical behaviour between WILMES-HE and WINSAUER-HE FTS was not statistical significant (*P* = 0.845–0.997) up to 6 mm of loading (Table 1b). Despite great deformation of single wires and OMIs of the three standard FTSs, the abutment attachments remained stable up to maximum static loading.

In the second equivalent series of tests, double wire arms (wires positioned 'side by side') were used as reinforced FTSs of the three HE types. At 1.0 mm of static lateral loading, the force values of these reinforced FTSs were between 110.0 (18,4) N and 134.8 (22.3) N without plastic deformation (Table 1c; Figure 3d and 3f). At 1 mm of static loading, the three reinforced (double wire) FTSs types reached without plastic deformation almost the same force values (82–98 %) which single wire FTSs only reached after 6 mm and under great plastic deformation of wires and OMIs.

Additional 2 mm (total of 3 mm) of static loading on the LUDWIG-HE double wire FTS increased the force from 110 (18.4) N to 209.2 (31.5) N with plastic deformation. If this gain of force represents approximately 100%, the additional final 3 mm of lateral feed (total of 6 mm) only increased the force once more by 51.7 N [total 260.9 (44.0) N] yet increasing plastic deformation to a major extent. These final 3 mm (total 6 mm) only represent additional 24.9% of force increase, hence needing the double amount of feed of static loading.

The force gain between 1 and 3 mm of lateral loading on the WINSAUER-HE FTS with reinforced (double wire) arm resulted in 271.3 (31.8) N with plastic deformation of wires and OMIs. If this represents 100% of force gain, the additional final 3 mm of feed (total 6 mm) increased the force to 320.9 (31.1) N, representing only additional 18.2% (Table 1c; Figure 5c). Up to 3 mm, there is no statistical difference in mechanical behaviour between WINSAUER-HE FTS and WILMES-HE FTS (*P* = 0.417).

The original abutment of the reinforced (double wire) WILMES-HE FTS detached between 3.0 and 3.9 mm of lateral feed which likewise interrupted the transfer of forces and moments making further measurements impossible (Table 1d and 1e; Figure 5a and 5d). Using reinforced FTS, both bonded abutments (LUDWIG-HE and WINSAUER-HE) could be loaded up to 6 mm reaching forces between 250 N and 300 N without detachment but showing great deformation of OMIs and double wires (Figure 5b–d; Table 1c).

The WINSAUER-HE OMI shaft had the greatest inner diameter (Table 2) and deformed least (10° less compared to LUDWIG-HE OMI) during the full range of 6 mm of loading with the reinforced FTS. In this test, the OMI experienced a slight rotation around its fulcrum [Table 1d (d1); Table 1e (α1, α2)]. The WINSAUER-HE abutment attachment withstood a 19% higher loading force than the one of LUDWIG-HE (Figure 5d). The screw-fixated WILMES-HE FTS abutment attachment (only partially overlapping) detached around 250 N. The bonded
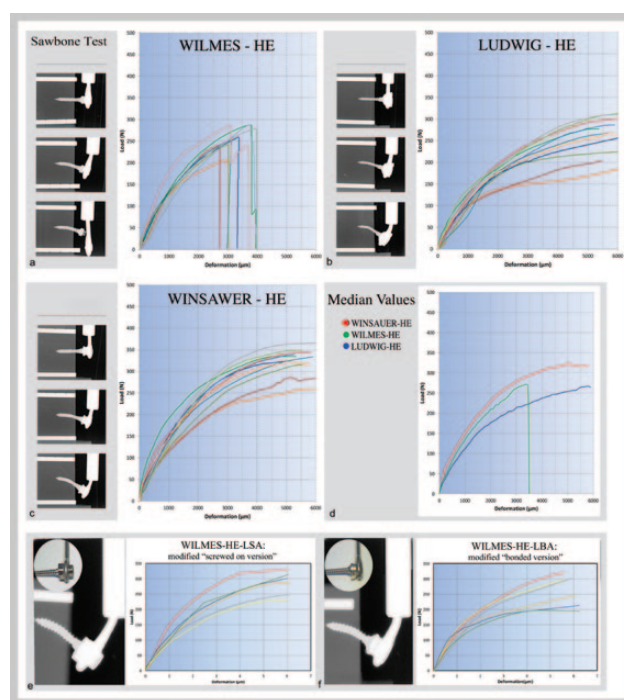
Figure 5. X-ray images and results of the force-transmitting system (FTS) tests at 0, 3 and 6 mm of static loading (a–c) in artificial bone blocks. All tests performed with double wire specimens. (a) Test of WILMES-HE OMI with its inner screw-fixated (original) PSM abutment attachment. (b) Test of LUDWIG-HE OMI with its bonded original abutment attachment. (c) Test of WINSAUER-HE OMI with bonded Tiger Dental abutment attachment. (d) Mean force values during continuous 6 mm of static loading of the three FTS. (e) Test with WILMES-HE OMI and modified lengthened inner screw-fixated abutment attachment (LSA). (f) Test with WILMES-HE OMI and modified lengthened bonded abutment attachment (LBA). HE = hybrid expander; OMI = orthodontic mini-implant.

LUDWIG-HE and WINSAUER-HE abutment attachments and a modified bonded plus a modified screw-fixated WILMES-HE abutment attachment overlapped 89–100 % without detaching (Tables 1c and 2).

SEM measurements showed that the three OMIs differed in shape, length and width (Table 2). The original WILMES-HE abutment attachment overlapped the OMI head by only 34%, while the two bonded abutments covered the OMI heads by 100% (Table 2). In the variable control test, the WILMES-HE-LSA (screwed on version, #1) and the WILMES-HE-LBA (bonded version, #2) of the modified WILMES-HE samples overlapping 100% did not detach under maximum loading [289 N (#1), 299 N (#2); Table 3; Figure 3e and 3f]. In the first 3 mm of static loading, no statistical differences (Table 3) were found between the original WILMES-HE abutment attachment (34% overlapping) and the 100% overlapping WILMES-HE-LSA and WILMES-HE-LBA, although the differences become evident beyond 3 mm. The mechanical behaviour between the WILMES-HE-LSA and the WILMES-HE-LBA showed no statistical differences during loading up to 6 mm (Table 3).

Discussion

Single versus double wire arm

It is important to point out that only the anterior bone-borne force-transmitting arm of a maxillary expander was tested. As maxillary expansion appliances consist of an anterior and a posterior force-transmitting arm, hypothetically the available expansive force of the

Table 3. Comparison of modified WILMES-HE abutment versions versus original WILMES-HE version (in double wire FTS). FTS = force-transmitting system; LSA (modified WILMES-HE abutment attachment) = lengthened screw-fixated abutment attachment; LBA (modified WILMES-HE abutment) = lengthened bonded abutment attachment.

			P-values*		
Original mean (SD) of Newtons	LSA mean (SD) of Newtons	LBA mean (SD) of Newtons	Original versus LSA	Original versus LBA	LSA versus LBA
130.6 (18.9)	127.0 (10.7)	129.5 (15.9)	0.908	0.999	0.942
254.2 (23.6)	235.5 (22.1)	238.0 (33.1)	0.367	0.467	0.985
—	289.7 (30.9)	299.0 (34.4)	—	—	0.632

The 6 mm values were calculated with a Student's *t*-test for independent samples.

*P-values were calculated using a Tukey's multiple comparison correction in ANOVA, except data at 6 mm values.

anterior standard single wire FTS arm in this *in vitro* study could be doubled in order to implement the potentially available total expansion force for clinical considerations.

Our results show that the maximum loading capacity of the anterior FTS with a single standard wire bone-borne arm reaches values between 63 N and 75 N without deformation. Therefore, the maximum overall unilateral force delivery without plastic deformation of the standard anterior and posterior FTS of a single wire hyrax screw could be estimated between 126 N and 152 N.

In clinical use with a tooth-borne single wire arm expander, Isaacson *et al.* (22) recorded 100 N as maximum force in a 15.6-year-old girl. The other four patients were younger and needed lower forces. In another similar clinical study of 10 patients (age 9–13 years), the maximum forces for suture opening were recorded around 120 N (23).

The present study shows that standard single wire FTSs generally used in todays hyrax expanders may suffice for RME in children and young adolescents but are questionable in young or more mature adults (23). In today's rapid maxillary expansion appliances, expansion screws with single 1.5 mm wire arms are used routinely. There are no expansion screws with greater wire diameter and therefore greater stability commercially available. Adding a second wire or using greater diameters wires would provide more stability and withstanding force.

Testing the reinforced (double wire) FTSs force values without plastic deformation between 110 N and 135 N were reached. As maxillary expanders consist of two FTSs per side, values between 220 N and 270 N could be estimated as possible total expansive force. This is nearly double the force of a single wire HE expander and taking plastic deformation of connecting double wire arms (positioned side by side) into account the expansion force of the anterior and posterior FTS together may well be up to 500 N (Table 1b).

Muchitsch *et al.* (17) have studied the stiffness of single and double 1.5 mm crude wire arms. F_{max} of double arms positioned 'side by side' was 2.53 times greater than that of a single wire. If double wires positioned 'one on top of each other and welded together at both ends' were loaded, F_{max} was 3.38 times greater than that of a single wire arm. They suggest that for use in adolescents the clinical setting should contain only double wire arms positioned as mentioned above.

In our three-point expansion screw flexural test (Figure 4b) with wires positioned 'on top of each other', expansion forces up to 438 N were enabled without deformation (Table 1a; Figure 4c). Our wires were not only laser welded at their ends but entirely lengthwise. This may explain why the results of our double wire bending pretest with wires positioned 'on top of each other' differ to the above findings and are close to 4.9 times greater than with a single standard wire

(all without plastic deformation). Under plastic deformation, more than 700 N of total expansion force is possible (Figure 4b and 4c).

Bending and shearing forces

Boryor *et al.* (24) placed their expander in a 73-year-old female cadaver directly on top of the bone after removing the palatal mucosa. During initial suture opening with a pure bone supported palatal expander (4 OMIs, Forestadent 1.7 mm diameter × 8 mm length) a force of 85 N was registered (24). Lee *et al.* (25) have used a similar set-up in a 3D finite element stress distribution analysis, finding the highest stress distribution located in the midpalatal suture. However, these set-ups involved 4 OMIs and exerting forces confined essentially to the plane of resistance of the OMIs where only minimal moments were present. This situation does not reflect the clinical use of orthodontic expanders. In a narrow palate, the expansion screw must be placed more occlusally and therefore lies more distant from the centre of resistance. The OMIs used in HEs in the present study therefore represent a cantilever arm of around 8 mm (2 mm head and neck portion, 3 mm upper shank section in the palatal mucosa (19) and 3 mm lower shank section until the OMIs centre of resistance; Figures 1g and 2a). The strongest reinforced (double wire) FTS withstood in our test 134 N without deformation. This corresponds to a calculated moment of 1072 N mm (Force × lever arm) (26) (Figure 2a). Ideally the expansion screw and every component of the FTS (wire arm, abutment attachment and OMI) should withstand these moments without major deformation (Figures 3f, 4b and 4c). A solid structural design of the expansion screw and its adjacent FTS components is obligatory in order to counteract these moments during successful maxillary expansion in more mature patients. Adding an additional wire and using OMIs of greater diameter than 2.0 mm to reinforce maxillary expanders in order to fulfil the upper requirements has been exercised several times by the authors. This arrangement of the wires and OMIs is easy to implement and has met the requirements in pure bone-borne expanders when used in more mature patients (8) (Figure 1o).

The bending (plastic deformation) of both the double wire arm and the OMI shaft as a reaction of not sufficient counter moment production are shown in Figure 5b, 5c, 5e and 5f. In all these tests, the OMI shaft bent in direction of the force applied (convex shape due to bending force; Table 1c and 1d; Figure 6a). This represents the bending behaviour of the OMI shaft when the attached wire arms (single or double) deform. In order to clarify which of the two variables—the wire arm or the OMI shaft—were the determinant variable for deformation, we replaced the double wire arm by the 6 mm power arm of the Galdabini machine (calculated stiffness exceeding
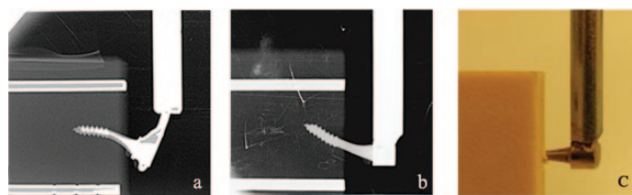
Figure 6. Mechanical behaviour after static loading using FTSs with different component characteristics. (a) WINSAUER-HE OMI with its collar abutment connected with double wire arms to the power arm of the testing machine. OMIs head bent laterally (CONVEX deformation, BENDING force). (b) WINSAUER-HE OMI with its collar abutment directly laser welded to the power arm. OMIs shaft tip bending inward (CONCAVE deformation, SHEAR force). (c) Image of the exploratory test set-up. HE = hybrid expander; OMI = orthodontic mini-implant.

that of the double wire arms by the factor 8). In an exploratory test (*n* = 1), the WINSAUER-HE abutment attachment containing the bonded OMI was directly laser welded to this power arm and in this setting the OMI bent after 6 mm of lateral loading to the opposite direction (concave shape due to shear force) reaching 391 N (Figure 6b and 6c). In this setting, the force value exceeded the values with single wire arms [mean 158.3 (12.4) N, *n* = 6] by 232.7 N or 147% (!). Compared to the double wire FTS arms [mean 320.9 N (31.1) N, *n* = 10], this directly laser welded setting developed only 70.1 N or 21.8% more force. This proves that in this setting the single wire arm is by far the weakest point within the force transmission system due to lack of stability and therefor not capable to withstand the arising moments. For better understanding—no matter if an OMI like in Figure 6c has a thin shaft diameter or a shaft with great diameter—there will always be concave shape deformation of the shaft when loaded laterally without a deforming element in between.

Abutment attachments

In the static loading test, the two bonded abutment attachments (LUDWIG-HE and WINSAUER-HE) and the modified WILMES-HE-LSA and the WILMES-HE-LBA withstood all applied counteracting moments and appear to be the most reliable components of the FTSs.

Orthodontic mini-implants

The greater the shank diameter (Table 2) and the harder the alloy of an OMI, the less it will deform and the more it will withstand lateral loading force during expansion (Figure 5c). This explains why the thinner LUDWIG-HE OMI shaft deformed more even under less lateral loading than the other OMIs (Table 1e; Figure 5b).

In the present test, we had inserted the OMIs at a depth of 8 mm, which seldom reflects the ideal clinical reality. In our clinical experience, the average insertion depth in the lateral anterior palate in position M4 is between 4 and 8 mm (15). The bending effect in the OMIs shaft occurs, when the force-transmitting wire arm shows early deformation presupposed the insertion depth of the OMI is deep enough and stable. Thus, in order to improve the bony anchorage and the stability of the OMIs, thicker shafts (2.5–3 mm) should be used, as there is sufficient space and bone depth in the anterior palatal region. A previous study showed clearly that the OMI characteristics, especially the inner to outer diameter ratio significantly affect primary stability and the risk of OMI fracture (21). An increase of the OMI inner diameter of only 0.1 mm already significantly improved torsional fracture values. Furthermore, it had been demonstrated that the maximum von Mises stress in peri-implant

cortical bone manifested on the outer most external surface (27). Wehrbein *et al.* (4) introduced the Orthosystem with an osseointegrated dental implant in the anterior palate of 3.3 mm diameter and a length of 6 mm, which could be an alternative option. Winsauer (8) has introduced an expansion appliance (MICRO-4/6 expander) that uses 4 or 6 OMIs with 2.5 mm diameter as a pure bone-borne anchorage for maxillary expansion without any dental side effects (Figure 10). Although the time of suture ossification varies greatly, there is no doubt that adults will generally require higher forces than adolescents (28). Thus, the bone-borne expanders can be a viable treatment option, since the forces can be directly applied to the basal bone and therefore the amount of skeletal effect of treatment may increase (24, 25).

Tremendous deformations of the FTS with standard single wire arms and therefore tipping and deformation of wire arms and adjacent OMIs at a force of only 120 N may indicate a putative weakness in the design and construction of today's HEs when used in more mature patients (Table 1b). Todays standard tooth-borne RME expanders and standard HEs only use single wire arms as the connection between the expansion screw and the teeth or the OMIs. These single wire arm FTSs are not adequate in counteracting forces exceeding 63–76 N without deforming. If, like in older adolescents and adults, expansion forces of more than 120 N are required, double wire fixation arms in HEs must be mandatory not showing deformation under lateral loading until 220–270 N.

Limitation of the study

The findings of this study are based on ideal settings presenting values that might not be reached in clinical reality in terms of insertion depth or bone density.

Conclusion

Double wires (ideally positioned 'on top of each other') should be used obligatory in HEs for elder patients with a more mature bony situation. Ideally no wires but only abutment attachments laser welded directly to the expansion screw body are optimal (i). Bonded and internal screw-fixated abutment attachments are stable and reliable up to 250 N (ii). A complete overlapping of the abutment on the screw head avoids early detachment during maximum lateral loading (iii). For higher loads, OMIs with inner shank diameters greater than 1.36 mm should be mandatory as they deform less (iv). As the tested double wire arm FTS demonstrated great stability, pure bone-borne expanders with such reinforced FTSs may represent a viable option, as they have no dental side effects (v).

References

1. Timms, D.J. (1997) Emerson C. Angell (1822–1903). Founding father of rapid maxillary expansion. *Dental Historian: Lindsay Club Newsletter*, 32, 3–12.
2. Haas, A.J. (1961) Rapid expansion of the maxillary dental arch and nasal cavity by opening the midpalatal suture. *The Angle Orthodontist*, 31, 73–90.
3. Muchitsch, A.P., Winsauer, H., Wendl, B., Pichelmayer, M., Kuljuh, E., Szalay, A. and Muchitsch, M. (2012) Remodelling of the palatal dome following rapid maxillary expansion (RME): laser scan-quantifications during a low growth period. *Orthodontics and Craniofacial Research*, 15, 30–38.
4. Wehrbein, H., Glatzmaier, J., Mundwiller, U. and Diedrich, P. (1996) The Orthosystem–a new implant system for orthodontic anchorage in the palate. *Journal of Orofacial Orthopedics = Fortschritte der Kieferorthopädie:*

Organ/official journal Deutsche Gesellschaft für Kieferorthopädie, 57, 142–153.

5. Ludwig, B.G., Zorkun, B., Wilmes, B., Kinzinger, G. and Lisson, J. (2009) Forcierte Gaumennahterweiterung mit skelettalem Kraftansatz: die Hybrid-GNE. *Kieferorthop*, 23, 267–274.

6. Wilmes, B. and Drescher, D. (2008) A miniscrew system with interchangeable abutments. *Journal of Clinical Orthodontics: JCO*, 42, 574–580; quiz 595.

7. Wilmes, B., Nienkemper, M. and Drescher, D. (2010) Application and effectiveness of a mini-implant- and tooth-borne rapid palatal expansion device: the hybrid hyrax. *World Journal of Orthodontics*, 11, 323–330.

8. Winsauer, H., Vlachojannis, J., Winsauer, C., Ludwig, B. and Walter, A. (2013) A bone-borne appliance for rapid maxillary expansion. *Journal of Clinical Orthodontics: JCO*, 47, 375–381; quiz 388.

9. MacGinnis, M., Chu, H., Youssef, G., Wu, K.W., Machado, A.W. and Moon, W. (2014) The effects of micro-implant assisted rapid palatal expansion (MARPE) on the nasomaxillary complex–a finite element method (FEM) analysis. *Progress in Orthodontics*, 15, 52.

10. Lagravère, M.O., Carey, J., Heo, G., Toogood, R.W. and Major, P.W. (2010) Transverse, vertical, and anteroposterior changes from bone-anchored maxillary expansion vs traditional rapid maxillary expansion: a randomized clinical trial. *American Journal of Orthodontics and Dentofacial Orthopedics: official publication of the American Association of Orthodontists, its constituent societies, and the American Board of Orthodontics*, 137, 304.e1–e12; discussion 304–305.

11. Baumgaertel, S. (2009) Quantitative investigation of palatal bone depth and cortical bone thickness for mini-implant placement in adults. *American Journal of Orthodontics and Dentofacial Orthopedics: official publication of the American Association of Orthodontists, its constituent societies, and the American Board of Orthodontics*, 136, 104–108.

12. Gracco, A., Lombardo, L., Cozzani, M. and Siciliani, G. (2008) Quantitative cone-beam computed tomography evaluation of palatal bone thickness for orthodontic miniscrew placement. *American Journal of Orthodontics and Dentofacial Orthopedics: official publication of the American Association of Orthodontists, its constituent societies, and the American Board of Orthodontics*, 134, 361–369.

13. Kang, S., Lee, S.J., Ahn, S.J., Heo, M.S. and Kim, T.W. (2007) Bone thickness of the palate for orthodontic mini-implant anchorage in adults. *American Journal of Orthodontics and Dentofacial Orthopedics: official publication of the American Association of Orthodontists, its constituent societies, and the American Board of Orthodontics*, 131(Suppl. 4), S74–S81.

14. Lai, R.F., Zou, H., Kong, W.D. and Lin, W. (2010) Applied anatomic site study of palatal anchorage implants using cone beam computed tomography. *International Journal of Oral Science*, 2, 98–104.

15. Winsauer, H., Vlachojannis, C., Bumann, A., Vlachojannis, J. and Chrubasik, S. (2014) Paramedian vertical palatal bone height for mini-implant insertion: a systematic review. *European Journal of Orthodontics*, 36, 541–549.

16. Nienkemper, M., Wilmes, B., Pauls, A. and Drescher, D. (2012) Multipurpose use of orthodontic mini-implants to achieve different treatment goals. *Journal of Orofacial Orthopedics = Fortschritte der Kieferorthopädie: Organ/official journal Deutsche Gesellschaft für Kieferorthopädie*, 73, 467–476.

17. Muchitsch, A.P., Wendl, B., Winsauer, H., Pichelmayer, M. and Payer, M. (2011) Rapid maxillary expansion screws on the test bench–a pilot study. *European Journal of Orthodontics*, 33, 256–262.

18. Petrey, J.S., Saunders, M.M., Kluemper, G.T., Cunningham, L.L. and Beeman, C.S. (2010) Temporary anchorage device insertion variables: effects on retention. *The Angle Orthodontist*, 80, 446–453.

19. Lee, Y.J., Kwon, Y.H., Park, J.B., Herr, Y., Shin, S.I., Heo, S.J. and Chung, J.H. (2010) Epithelial thickness of the palatal mucosa: a histomorphometric study in Koreans. *Anatomical Record*, 293, 1966–1970.

20. Devlin, H., Horner, K. and Ledgerton, D. (1998) A comparison of maxillary and mandibular bone mineral densities. *The Journal of Prosthetic Dentistry*, 79, 323–327.

21. Walter, A., Winsauer, H., Marcé-Nogué, J., Mojal, S. and Puigdollers, A. (2013) Design characteristics, primary stability and risk of fracture of orthodontic mini-implants: pilot scan electron microscope and mechanical studies. *Medicina Oral, Patología Oral y Cirugía Bucal*, 18, e804–e810.

22. Isaacson, R.J., Wood, J.L. and Ingram, A.H. (1964) Forces produced by rapid maxillary expansion. Part I. Design of the force measuring system. *The Angle Orthodontist*, 34, 256–260.

23. Sander, C., Hüffmeier, S., Sander, F.M. and Sander, F.G. (2006) Initial results regarding force exertion during rapid maxillary expansion in children. *Journal of Orofacial Orthopedics = Fortschritte der Kieferorthopädie: Organ/official journal Deutsche Gesellschaft für Kieferorthopädie*, 67, 19–26.

24. Boryor, A., Hohmann, A., Wunderlich, A., Geiger, M., Kilic, F., Kim, K.B., Sander, M., Böckers, T. and Sander, C. (2013) Use of a modified expander during rapid maxillary expansion in adults: an in vitro and finite element study. *The International Journal of Oral & Maxillofacial Implants*, 28:e11–e16.

25. Lee, H.K., Bayome, M., Ahn, C.S., Kim, S.H., Kim, K.B., Mo, S.S. and Kook, Y.-A. (2014) Stress distribution and displacement by different bone-borne palatal expanders with micro-implants: a three-dimensional finite-element analysis. *European Journal of Orthodontics*, 36, 531–540.

26. Byloff, F.K. and Mossaz, C.F. (2004) Skeletal and dental changes following surgically assisted rapid palatal expansion. *European Journal of Orthodontics*, 26, 403–409.

27. Duaibis, R., Kusnoto, B., Natarajan, R., Zhao, L. and Evans, C. (2012) Factors affecting stresses in cortical bone around miniscrew implants: a three-dimensional finite element study. *The Angle Orthodontist*, 82, 875–880.

28. Knaup, B., Yildizhan, F. and Wehrbein, H. (2004) Age-related changes in the midpalatal suture. A histomorphometric study. *Journal of Orofacial Orthopedics = Fortschritte der Kieferorthopädie: Organ/official journal Deutsche Gesellschaft für Kieferorthopädie*, 65, 467–474.